

Strange Effects of Pulse Shaping in Water Presaturation Experiments

Eriks Kupče* and Ray Freeman†

*Varian NMR Instruments, 28 Manor Road, Walton-on-Thames, Surrey, KT12 2QF, England; and †Department of Chemistry, University of Cambridge, Lensfield Road, Cambridge CB2 1EW, England

Received April 10, 2000; revised June 6, 2000

During the course of some water presaturation experiments with a shaped pulse envelope we observed inverted responses from certain signals flanking the water response. This phenomenon did not occur when a rectangular presaturation envelope was used. Apparently the leading and trailing edges of the shaped pulse act as adiabatic sweeps, causing the coupled magnetizations in question to be spin-locked. This gives rise to Hartmann–Hahn coherence transfer, and when the spin lock duration is equal to $1/(2J)$ the trajectories are such as to carry these magnetization vectors to the $-z$ axis, leading to inverted signals in the final spectrum. © 2000 Academic Press

We report here an NMR phenomenon that might appear at first sight to be paradoxical—that an apparently trivial modification of a pulse envelope completely alters what is observed. We have recorded inverted responses from certain proton sites in an otherwise conventional absorption-mode spectrum obtained under conditions that would rule out Overhauser effects or chemically induced nuclear polarization. These experiments involved a modified form of water presaturation.

Most of the present-day applications of high-resolution proton NMR are in the biochemical field, and in many cases these macromolecules must be studied in aqueous solution, not in heavy water. Hence the importance of water suppression techniques to counter the dynamic range problem. Presaturation has become a popular method, irradiating the water resonance with a continuous radiofrequency field just prior to initiation of the pulse sequence proper. The accepted practice is to keep the irradiation field strength B_1 at a modest level in order to avoid collateral saturation of signals near the water line. We were exploring the possibility of using an appreciably shorter period of preirradiation with a correspondingly more intense radiofrequency field in order to speed up the data gathering and hence improve sensitivity per unit time. The basic idea was to reduce attenuation of signals close to water by shaping the leading and trailing edges of the irradiation envelope to act as adiabatic sweeps. The “tailored” leading edge carries off-resonance magnetization from the $+z$ axis to the direction of the effective field, where it remains spin-locked for most of the preirradiation period. Then the shaped trailing edge returns these magnetizations to the $+z$ axis. The water signal (at exact reso-

nance) does not experience any adiabatic sweep but merely a B_1 field of varying amplitude. Related schemes have been used in certain modifications of the ROESY technique (1, 2) to reduce the contributions from coherence transfer (3, 4).

The shaping envelope used for these experiments was one of the family of WURST functions (5) defined by

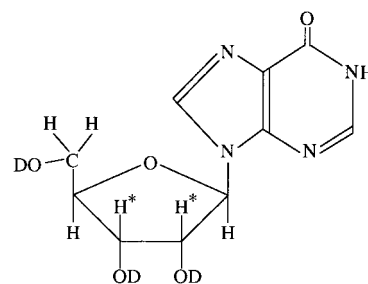
$$B_1 = B_1^0 \{1 - \sin(\beta t)^k\}, \quad [1]$$

where k is an even integer and $-\pi/2 < \beta t < \pi/2$. It ensures that the adiabatic condition (6) is reasonably well satisfied:

$$|d\theta/dt| \ll \gamma B_{\text{eff}}. \quad [2]$$

This implies that the inclination θ of the effective field changes slowly with respect to its intensity B_{eff} expressed in frequency units. Minor violation of the adiabatic condition leads to low-amplitude oscillations about the effective field which accelerate as B_{eff} increases.

We tested this idea on the proton NMR spectrum from an aqueous solution of inosine



SCHEME 1

recorded at 500 MHz and 28.5°C. The envelope of the presaturation pulse had a maximum radiofrequency level given by $\gamma B_1/2\pi = 2.2$ kHz and a duration of 100 ms, and was shaped according to the WURST recipe (5) with $k = 2$. The relevant section of the conventional high-resolution spectrum is shown in Fig. 1a with the intense water signal truncated at 4%. With the normal rectangular presaturation envelope, all proton res-

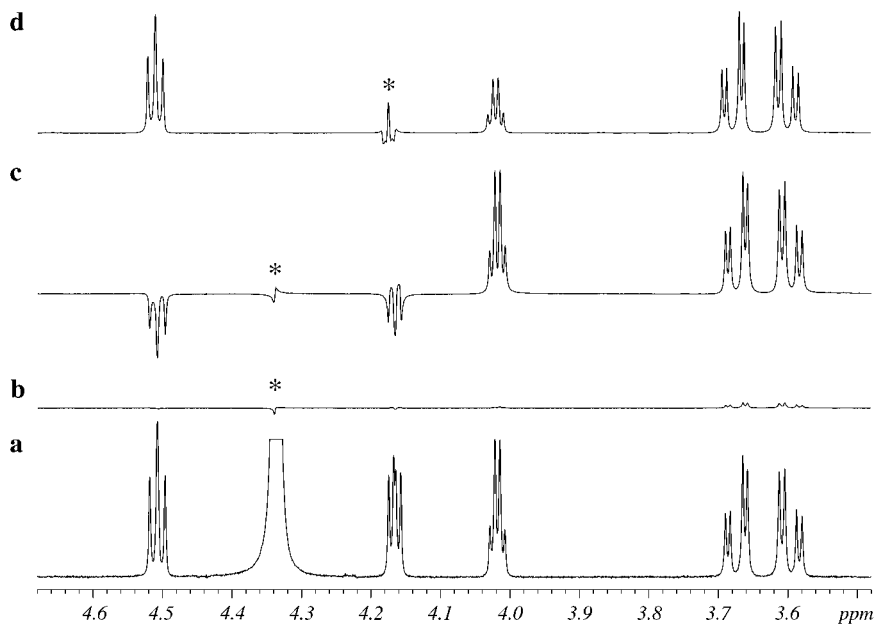


FIG. 1. (a) A section of the 500-MHz proton NMR spectrum of an aqueous solution of inosine (Scheme 1). The intense water signal has been truncated at 4%. (b) The same after presaturation of water (*) with 100 ms of intense irradiation with a rectangular envelope. All the nearby resonances are also saturated. (c) The same except that the leading and trailing edges of the irradiation pulse were rounded off with a WURST shaping function (see text). Although collateral saturation of neighboring resonances has been avoided, there is an unanticipated distortion of the two responses nearest to water (at 4.16 and 4.51 ppm). (d) Spectrum recorded at 40.0°C where the water signal (*) and the irradiation frequency are shifted to 4.16 ppm. The response at 4.51 ppm is now restored to its usual upright form.

onances in the vicinity of water were also saturated, as expected (Fig. 1b). When the shaped presaturation envelope was employed, these close neighbors were far less affected (Fig. 1c). This avenue of investigation is now being explored in detail, and we hope to publish a report in the near future.

However, a quite unexpected new phenomenon is evident in the spectrum shown in Fig. 1c. Two resonances that flank the water signal (from protons marked with an asterisk in Scheme 1) show *inverted* absorption-mode responses (with a small amount of dephasing), whereas the remainder of the spectrum is quite normal. Since these “rogue” responses belong to a coupled spin system, and happen to fall essentially symmetrically either side of the irradiation frequency, one immediately suspects a Hartmann–Hahn effect (7) as the culprit. This explanation is supported by the fact that when the temperature was raised to 45.0°C so that the water resonance (and its irradiation frequency) moved away from the mean chemical shift of these two sites, the normal upright response was observed for the low-field site, while the signal from the high-field site was so close to resonance that it was saturated (Fig. 1d). While we might hope that this was just a fortuitous case, we must bear in mind that in the thousands of biomolecular spectra under investigation, such a situation could reoccur with some regularity.

We set out to investigate this phenomenon in more detail using a “textbook” example of a first-order coupled two-spin system. This was the high-resolution proton NMR spectrum of

uracil in DMSO- d_6 recorded at 500 MHz. The conventional spectrum consists of two responses I and S, separated by 928 Hz, both doublets with $J_{IS} = 7.6$ Hz (Fig. 2a). In this example any residual HDO signal was too far distant to cause any interference in the spectral region under investigation.

The frequency of the preirradiation pulse was centered at the mean chemical shift of I and S. It had a rectangular envelope with a duration τ chosen to satisfy the condition for maximum Hartmann–Hahn interchange of coherence between two coupled spins

$$\tau = (2n - 1)/(2J_{IS}), \quad [3]$$

where n is an integer, in this case unity. An essentially zero response was detected from the two sites (Fig. 2b). This is hardly surprising, for three reasons. First of all, a continuous spin-lock field is designed to act on transverse magnetization but there is none at the beginning of the experiment. Secondly, a spatially inhomogeneous spin-lock field, acting on longitudinal magnetization over this relatively long time scale, would induce such an extensive dephasing of magnetization isochromats that no resultant signal would be detected. Thirdly, any Hartmann–Hahn coherence transfer in the liquid phase requires an imbalance between the I and S sites, whereas the initial state of this system is symmetrical with respect to I and S.

In complete contrast, when the leading and trailing edges of

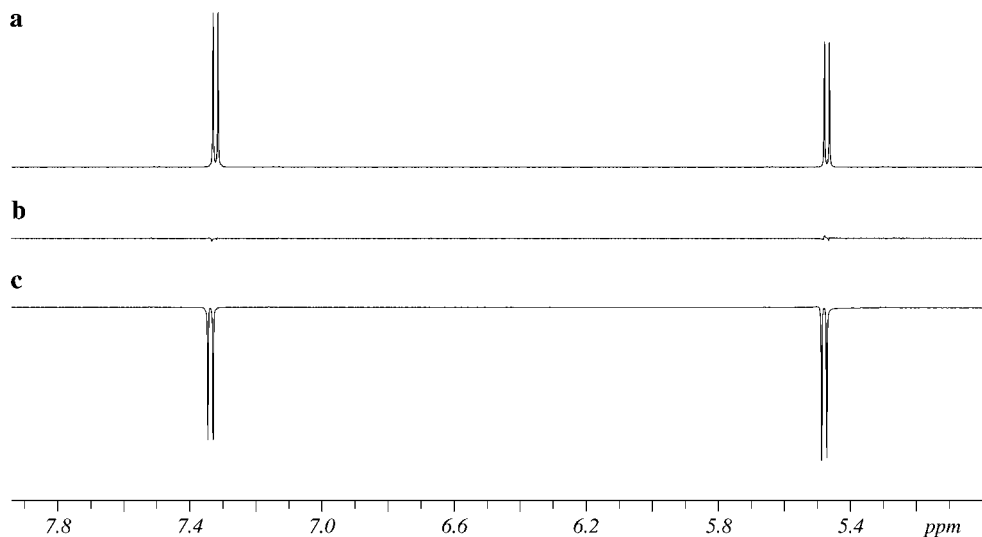


FIG. 2. (a) The conventional weakly coupled spectrum of uracil at 500 MHz showing the I doublet (left) and the S doublet (right). (b) An essentially zero response recorded under similar conditions except that a rectangular “presaturation” field was applied at the mid-point of the spectrum during a 66-ms preparation period. (c) A completely inverted spectrum recorded under similar conditions except that the presaturation envelope was rounded off at both extremities, keeping the period of full-intensity irradiation at 66 ms.

the spin-lock field were rounded off, an entirely different behavior was observed. Both sites now showed *inverted* absorption-mode signals (Fig. 2c), almost as intense as in the conventional spectrum, closely reminiscent of the results obtained with inosine in Fig. 1c. At first sight these observations might appear to be counterintuitive for it is not immediately obvious how this inversion comes about. Indeed one could be forgiven for thinking that because the preparation seems to be symmetrical with respect to I and S, no Hartmann–Hahn effect should occur.

The spectrum of Fig. 2c is the extreme case of inversion. The time evolution of the signal as a function of τ exhibits the cyclic behavior illustrated in Fig. 3. At short τ intervals a “conventional” upright absorption spectrum is observed, but as τ is increased the doublets evolve into antiphase dispersion, later becoming inverted absorption, with maximum inversion under the condition defined by Eq. [3], neglecting the short shaped sections of the pulse profile. After a complete cycle ($\tau = 1/J$) the initial upright form of the spectrum is restored. Note the clear distinction with respect to the usual liquid-phase

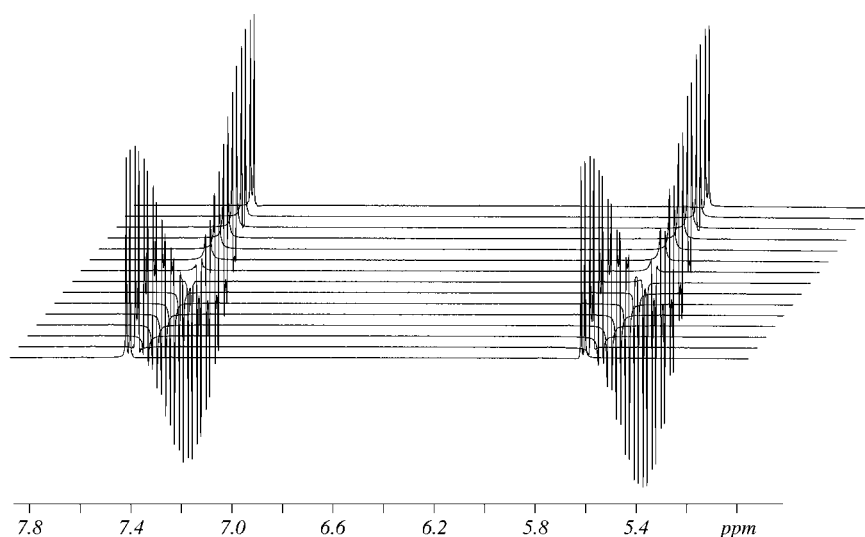


FIG. 3. Evolution of the uracil spectrum as a function of the duration τ of the preirradiation pulse, which runs from 150 to 290 ms in 10-ms steps. The leading and trailing edges of the irradiation envelope have been shaped with a WURST function with $k = 20$, and act as adiabatic sweeps. Hartmann–Hahn interchange of coherence occurs, giving inverted signals at $\tau = 220$ ms, and upright signals again at $\tau = 290$ ms.

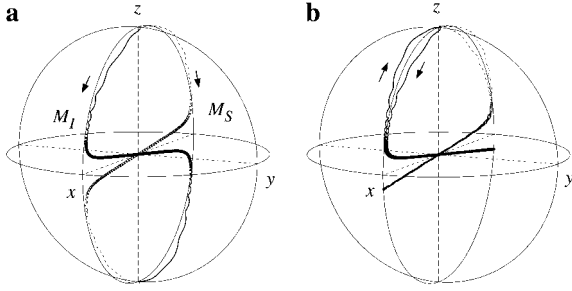


FIG. 4. (a) Simulation of the trajectories of \mathbf{M}_I (solid curves) and \mathbf{M}_S (dashed curves) during a presaturation period with shaped leading and trailing edges. The leading edge of the envelope acts as an adiabatic sweep, but because the resonance offsets of I and S are opposite in sign, \mathbf{M}_I moves toward $+x$, whereas \mathbf{M}_S moves toward $-x$. Because the B_1 field is finite, the two trajectories do not quite reach the $\pm x$ axes. Hartmann–Hahn coherence transfer with $\tau = 1/(2J)$ induces the crossover, leaving \mathbf{M}_I aligned approximately along $-x$, and \mathbf{M}_S approximately along $+x$. The shaped trailing edge of the envelope acts as a second adiabatic sweep, turning both \mathbf{M}_I and \mathbf{M}_S toward the $-z$ axis, giving an inverted spectrum. The small oscillatory motions reflect a slight violation of the adiabatic condition. (b) Corresponding trajectories for $\tau = 1/J$. The doubling of the spin-lock interval allows \mathbf{M}_I and \mathbf{M}_S to retrace their paths, and the final adiabatic sweep takes them on mirror-image trajectories back to the $+z$ axis, giving an upright spectrum.

homonuclear Hartmann–Hahn experiment where the I and S signals have *opposite* phases throughout.

The leading edge of the shaped spin-lock envelope acts as an adiabatic B_1 amplitude sweep (note that no *frequency sweep* is involved here). The magnetization vector \mathbf{M}_I , initially along $+z$, remains aligned with its effective field throughout the adiabatic sweep. As B_1 is increased from zero, \mathbf{M}_I rotates counterclockwise from the $+z$ axis to a position close to $+x$ as the spin-lock field reaches its peak value, $B_1 \gg |\Delta B|$. In contrast, \mathbf{M}_S remains *opposed* to its effective field (because ΔB is negative) and rotates *clockwise* from $+z$ to a position close to the $-x$ axis. In a certain sense the adiabatic sweep acts as a self-calibrating pulse, with a flip angle close to -90° for I, and close to $+90^\circ$ for S. The trailing edge of the shaped pulse induces analogous rotations in reverse as B_1 is swept from its maximum value to 0.

Figure 4a shows a simulation of the motion of \mathbf{M}_I and \mathbf{M}_S throughout the sequence. Although $B_1 \gg |\Delta B|$ at the end of the first adiabatic sweep, the rotation angles are rather less than 90° and the final orientations of \mathbf{M}_I and \mathbf{M}_S are not quite opposed; in practice θ reaches $\pm 84^\circ$. When the plateau of the irradiation is reached, Hartmann–Hahn transfer gradually moves \mathbf{M}_I to site S (where it experiences an effective field characteristic of that site) while \mathbf{M}_S is moved to site I (with its own characteristic effective field). The shaped trailing edge of the envelope acts as a second adiabatic sweep, but because \mathbf{M}_I and \mathbf{M}_S now experience interchanged effective fields, \mathbf{M}_I is rotated *clockwise* toward $-z$, whereas \mathbf{M}_S is rotated *counterclockwise* toward $-z$. The trajectories of \mathbf{M}_I and \mathbf{M}_S both reach the $-z$ axis without significant deviations. After a hard 90° pulse these population inversions are converted into negative-going ab-

sorption-mode signals, hence the surprising observation of a completely inverted IS spectrum.

The motion during Hartmann–Hahn coherence transfer can be represented in the product operator formalism (8) as

$$I_x - S_x \rightarrow (I_x - S_x)\cos(2\pi J\tau) + 2(I_y S_z - I_z S_y)\sin(2\pi J\tau), \quad [4]$$

assuming, for simplicity, an exactly opposed configuration of \mathbf{M}_I and \mathbf{M}_S at the start. The second term represents the antiphase dispersion-mode signals. If $\tau = 1/(2J)$, there is a maximum interchange between \mathbf{M}_I and \mathbf{M}_S . At this point the trailing edge of the spin-lock envelope acts as a reverse adiabatic B_1 sweep, imposing opposite senses of rotation on \mathbf{M}_I and \mathbf{M}_S , thus inverting both vectors.

If the spin-lock interval is doubled ($\tau = 1/J$), the same crossover of the I and S trajectories occurs, but this is then reversed, the I and S vectors following a return path that is an approximate mirror image of that at the beginning of the sequence (Fig. 4b). The vectors \mathbf{M}_I and \mathbf{M}_S are returned to the $+z$ axis and an upright spectrum is observed.

An interesting modification of this sequence employs a frequency-selective 90° read pulse, affecting only the S site. Consequently the I site receives no direct excitation but only an off-resonance (shaped) spin-lock field. If we observe an inverted response from \mathbf{M}_S near the condition $\tau = 1/(2J)$ this would indicate the presence of the coupled spin I, as if we could “see in the dark.” A practical application might be the indirect detection of the I response when it is hidden by overlying resonances, without disturbing the latter. This would rely on finding a suitable spin-lock frequency not too far from the optimum.

The actual results of this selective pulse experiment were rather surprising. The evolution of the S spin response follows the same cosine dependence as that observed in Fig. 3, but the signal remains in pure absorption throughout (Fig. 5a). The response at the I site consists of antiphase doublets that are always dispersive, with an amplitude that follows a sinewave dependence on the spin-lock duration. The trailing edge of the spin-lock envelope acts as a 90° pulse about the $-y$ axis for the I spins, but a 90° pulse about the $+y$ axis for the S spins, thus converting zero-quantum coherence into double-quantum coherence:

$$(I_x - S_x)\cos(2\pi J\tau) + 2(I_y S_z - I_z S_y)\sin(2\pi J\tau) \rightarrow (I_z + S_z)\cos(2\pi J\tau) + 2(I_y S_x + I_x S_y)\sin(2\pi J\tau). \quad [5]$$

The term $2I_x S_y$ is reconverted into antiphase single-quantum coherence by the selective $90^\circ(-x)$ pulse on the S spins:

$$(I_z + S_z)\cos(2\pi J\tau) + 2(I_y S_x + I_x S_y)\sin(2\pi J\tau) \rightarrow (I_z + S_y)\cos(2\pi J\tau) + 2(I_y S_x - I_x S_z)\sin(2\pi J\tau). \quad [6]$$

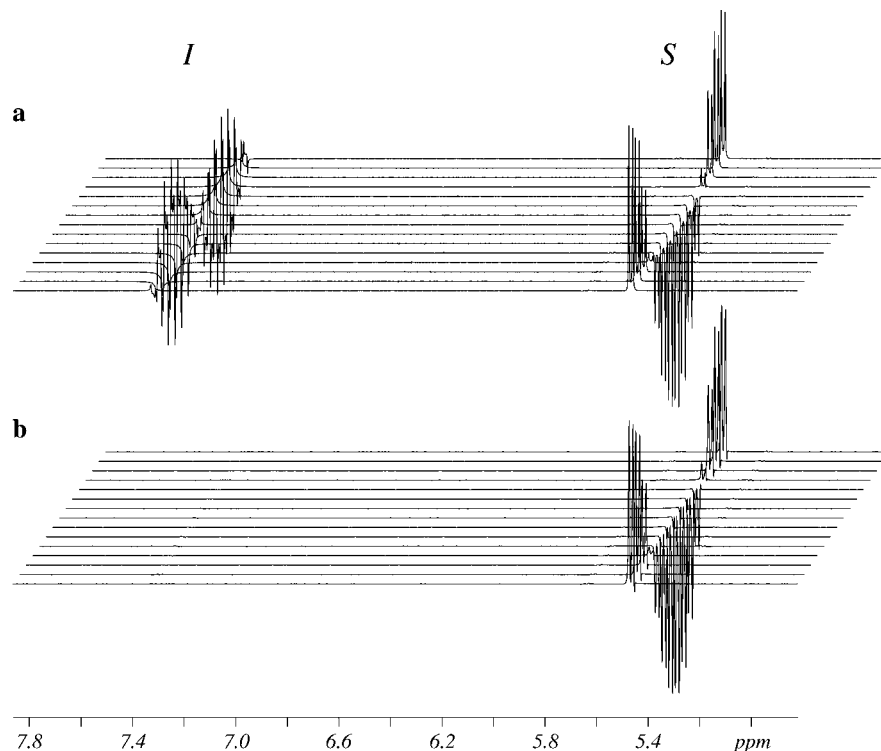


FIG. 5. Evolution of the uracil spectrum as a function of the spin-lock interval from $\tau = 150$ ms to $\tau = 290$ ms in 10-ms steps. (a) An experiment with a shaped irradiation field, followed by a *selective* 90° pulse applied to site S. (b) The same, except for the introduction of a purging magnetic field gradient just before the selective 90° pulse. Note the disappearance of the I spin response caused by dissipation of double-quantum coherence in the applied field gradient.

The only observable terms are a pure absorption signal $+S_y \cos(2\pi J\tau)$ from S and an antiphase dispersion signal $-2I_x S_z \sin(2\pi J\tau)$ from I, as observed in Fig. 5a.

This property of the second adiabatic sweep—the ability to convert zero-quantum coherence into double-quantum coherence—turns out to be quite useful. If a static field-gradient pulse is applied between the end of the spin-lock interval and the selective 90° pulse, the double-quantum term $2(I_y S_x + I_x S_y)$ is dissipated by the gradient, giving a vanishing resultant, and no response is observed at the I site at any point of the time evolution (Fig. 5b).

We conclude that in some relatively rare circumstances where the frequency of a shaped presaturation pulse falls close to the optimum for Hartmann–Hahn coherence transfer in a coupled spin system, severe distortions of the NMR signals can occur, even complete signal inversion in the extreme case. An explanation in terms of adiabatic sweeps and spin-locking

along an effective field is borne out by simulations and experimental tests on a coupled first-order spin system.

REFERENCES

1. A. A. Bothner-By, R. L. Stephens, J. Lee, C. D. Warren, and R. W. Jeanloz, *J. Am. Chem. Soc.* **106**, 811 (1984).
2. A. Bax and D. G. Davis, *J. Magn. Reson.* **63**, 207 (1985).
3. H. Desvaux, P. Berthault, N. Birlirakis, M. Goldman, and M. Piotto, *J. Magn. Reson. A* **113**, 47–52 (1995).
4. F. A. A. Mulder, R. A. de Graaf, R. Kaptein, and R. Boelens, *J. Magn. Reson.* **131**, 351–357 (1998).
5. E. Kupče and R. Freeman, *J. Magn. Reson. A* **115**, 273–276 (1995).
6. A. Abragam, “The Principles of Nuclear Magnetism,” Clarendon Press, Oxford (1961).
7. S. Hartmann and E. L. Hahn, *Phys. Rev.* **128**, 2042 (1962).
8. O. W. Sørensen, G. W. Eich, M. H. Levitt, G. Bodenhausen, and R. R. Ernst, *Prog. NMR Spectrosc.* **16**, 163 (1983).